Suppression of Flow Oscillations in a Vertical Bridgman Crystal Growth System

Paul Sonda, Andrew Yeckel, Jeffrey J. Derby, and Prodromos Daoutidis
Department of Chemical Engineering and Materials Science
University of Minnesota,
Minneapolis, Minnesota, 55455, USA.
daoutidi@cems.umn.edu

Abstract— **In this work, we consider the feedback control of flows in a vertical Bridgman crystal growth system. The vertical Bridgman process is used to grow single crystals for a wide array of applications, ranging from lasers to high-speed microelectronics to infrared sensors. We model the Bridgman system using conservation equations for energy and momentum and physically reasonable boundary and initial conditions. The Galerkin finite element method is used to spatially discretize this nonlinear, differential-algebraic equation set. We consider a prototypical Bridgman system experiencing a time-varying disturbance to its furnace temperature profile. A single-input single-output control system is considered for controller design. Proportional, proportional-integral, and input-output linearizing controllers are applied to the vertical Bridgman model to attenuate the flow oscillations. The volume-averaged flow kinetic energy is chosen as the single controlled output. The flows are controlled via rotation of the crucible containing the molten material. Simulation results show that nonlinear control is superior to P and PI control in the suppression of the flow oscillations.**

I. Introduction

The vertical Bridgman process is used to grow single crystals, for use as substrates in optoelectronic and sensing devices. To produce devices of suitable quality, it is necessary to grow low-defect single crystals of homogenous chemical composition. This task is made difficult by the complex coupling of heat, mass, and momentum transport inherent in the process. One processing issue that continues to challenge the crystal growth community is the occurrence of fine scale variations in composition, known as striations. These composition variations often cause undesirable variations in material and electronic properties. Crystal growth experiments by Kim, Witt, and Gatos [1] investigated the occurrence of striations in a vertical Bridgman system. It was found that for sufficiently intense flows, the melt exhibited periodic, time-varying behavior. It was then shown conclusively that these time-varying flows were directly related to the occurrence of striations.

In previous work [2], [3], we used detailed crystal growth models to numerically simulate the experimental system of Kim, Witt, Gatos. In the early stages of crystal growth, our numerical simulations predict the occurrence of large amplitude, two-frequency oscillations within the flow. In later stages of growth, the oscillatory behavior becomes more ordered with decreasing amplitude until finally the flows are steady with time. These simulations are in qualitative agreement with the experimental results of Kim, Witt, and Gatos. Demonstrating the appearance of periodic, time-varying flows in our model was an important first step in our study of crystal striations. The next step, the subject of this work, is the formulation and implementation of feedback control algorithms that will beneficially alter the fluid dynamical behavior within the system.

Despite the continuing need for improvement of Bridgman growth processes, there exists minimal work addressing the feedback control of the process. Batur et al. [4], [5], designed a transparent, multi-heating zone furnace for growth of lead bromide. The transparent furnace, in coordination with a video camera and real-time imaging software, allowed for the observation of the melt-crystal interface shape. Comparison of the observed interface shape to the desired shape provided an error signal, which was used to adjust the furnace temperature profile. Azuma et al. [6] developed an automatic feedback control system to maintain a constant temperature at the melt-crystal interface during the growth of silicon germanium. The position of the interface was automatically detected through *in-situ* monitoring via a charge-coupled-device camera, and the ampoule translation rate was the manipulated input. Schmachtl et al. [7] used ultrasonic waves to control the shape and velocity of the solid-liquid interface during the Bridgman growth of copper manganese.

In this work, we implement feedback controllers to control the molten flows in the vertical Bridgman system. There are many actuation techniques that could perceptibly affect the fluid dynamics and be feasibly implemented. Some possibilities include real-time adjustment of the thermal environment, the application of vibration, or the use of a magnetic field. This work examines the use of crucible rotation as the means for controlling flows in the vertical Bridgman system. Open-loop crucible rotation has been successfully applied to experimental vertical Bridgman systems [8] and has been the subject of simulation-based studies (see [9] and references therein). Our specific purpose is the use of crucible rotation to suppress flow oscillations. If achieved in practice, this would be a significant step towards the removal of striations in crystal growth processes. Proportional, proportional-integral and nonlinear, model-based controllers are synthesized and implemented within the framework of our crystal growth simulation code

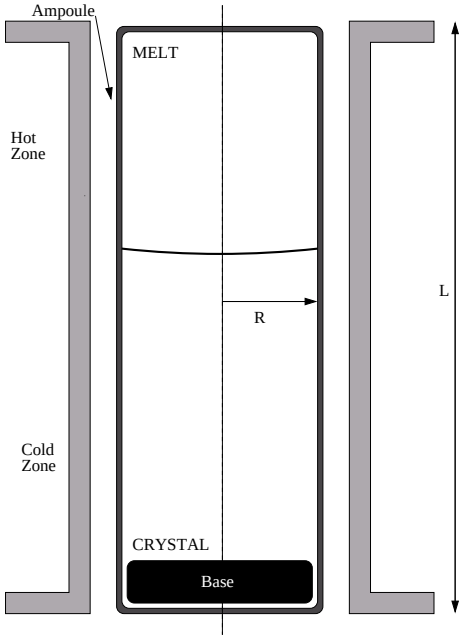

Fig. 1. Vertical Bridgman growth system studied in this work.

[10]. The controllers are applied to a vertical Bridgman system experiencing a time-oscillating disturbance and their performances evaluated.

II. PRELIMINARIES

A. The Vertical Bridgman Process Model

A schematic of the vertical Bridgman process is shown in Figure 1. Polycrystalline material is loaded into a quartz crucible (also known as an ampoule), inside of a high temperature furnace. The material is completely melted, at which time the distribution of temperature in the furnace is adjusted to vary along its length, such that one zone is hotter than the material's melting point and the other section is cooler. Directional solidification is achieved by slowly translating the crucible towards the cold zone of the furnace.

We use equations for conservation of mass, momentum, and energy, along with appropriate boundary and initial conditions, to model the vertical Bridgman system. Our present purposes only require that we study the effect of control on flow, so we do not include conservation of chemical species in the model, although doing so would be necessary for the direct prediction of striations. A key assumption used here is that the system is perfectly axisymmetric, in which case all field variables are independent of the azimuthal coordinate.

Under the these assumptions, the time-dependent energy transport equation is given by

$$Pr_m \frac{\partial T}{\partial t} + \mathbf{v} \cdot \nabla T - \nabla^2 T = 0 \quad (1)$$

in the melt, and

$$Pr_j \frac{\partial T}{\partial t} - \nabla^2 T = 0 \quad (2)$$

where the index j designates the material, either the crystal, crucible, or graphite support. T is a dimensionless temperature scaled by the melting temperature, T_{mp}, t is a dimensionless time scaled by R^2/ν, $\mathbf{v}$(r,z) is the dimensionless velocity field, and ∇ is the dimensionless gradient operator, in which the spatial coordinates are scaled by the crucible radius R. The Prandtl number is defined as $Pr_i \equiv \nu/\alpha_i$, where ν is the kinematic viscosity, and the thermal diffusivity is defined as $\alpha_i \equiv k_i/\rho_i C_{p,i}$, where k_i is the thermal conductivity, ρ_i is the density, and $C_{p,i}$ is the heat capacity.

The velocity field is described by the Navier-Stokes equations for incompressible flow, using the Boussinesq approximation to account for temperature-dependent density variation:

$$\nabla \cdot \mathbf{v} = 0 \quad (3)$$

$$\frac{\partial \mathbf{v}}{\partial t} + \frac{1}{Pr_m}\mathbf{v} \cdot \nabla \mathbf{v} - \nabla \cdot \mathsf{T} - Ra(T-1)e_z = 0 \quad (4)$$

Here the dimensionless velocity is scaled by α_m/R, T is the stress tensor, Ra is the Rayleigh number, $Ra \equiv g\beta_T R^3 T_{mp}/\nu\alpha_m$, where g is the gravitational constant, and β_T is the thermal expansivity, and e_z is the unit vector in the axial direction. The stress tensor is split up into the dynamic pressure and the strain rate tensor,

$$\top = -P\mathsf{I} - \tau = -P\mathsf{I} + (\nabla \mathbf{v} + \nabla \mathbf{v}^T) \quad (5)$$

where P is the dynamic pressure scaled by $\rho_m \nu \alpha_m / R^2$, and I is the idemfactor.

A thermal flux condition is defined at the melt-crystal interface,

$$-(\kappa \nabla T|_m + \nabla T|_s) \cdot \mathbf{n_{sm}} = StPr_s(\mathbf{n_{sm}} \cdot \dot{\mathbf{x}}) \quad (6)$$

where κ is the ratio of melt thermal conductivity to solid, $\kappa = k_m/k_s$, $\mathbf{n_{sm}}$ is the unit vector normal to the melt-crystal interface, pointed towards the melt, St is the Stefan number, $St = \Delta H_f / C_{p,s} T_{mp}$, and $\dot{\mathbf{x}}$ is the velocity of the melt-crystal interface.

The temperature at the melt-crystal interface is assumed to be equal to the material melting point,

$$T = 1. \quad (7)$$

We consider a vertical Bridgman system which experiences an external power disturbance, producing a time-varying furnace temperature profile,

$$T_f(z,t) = T_c + \left[\frac{(T_h - T_c)}{L}(z - z_r)\right](1 + \sin(wt)), \quad (8)$$

where T_f is the furnace temperature, T_c and T_h are the minimum and maximum furnace temperatures, respectively, z_r is the furnace reference position, and $w = 0.045$/s. Convective and radiative heat transfer from the furnace to the crucible are represented by a simple flux condition applied at the domain boundary:

$$-\nabla T|_a \cdot n_{af} = Bi_i(T - T_f(z)) + Rd_i(T^4 - T_f^4(z)) \quad (9)$$

where the Biot number, $Bi_i = hR/k_i$, is a dimensionless heat transfer coefficient, the Radiation number, $Rd_i = \sigma\epsilon_i RT_{mp}^3/k_i$, relates radiative effects to conductive effects, ϵ is the crucible emissivity, σ is the Stefan-Boltzmann constant, and n_{af} is the unit vector normal to the crucible/furnace interface. No-slip boundary conditions are assumed at the crucible walls and melt-crystal interface,

$$\mathbf{v} = \Omega r \mathbf{e}_\theta \tag{10}$$

where Ω is the crucible rotation rate and $\mathbf{e}_\theta$ is the unit vector in the azimuthal direction. Finally, at the centerline of the system, symmetry conditions are assumed.

The governing equations that comprise the model are nonlinear, coupled, partial differential equations. The Galerkin Finite Element Method (GFEM) was employed to spatially discretize equations for energy transport (Eq. 1), mass continuity (Eq. 3), and momentum transport (Eq. 4). This system of nonlinear DAEs was time integrated using a second-order implicit trapezoidal method, and the resulting system of nonlinear algebraic equations was solved using a modified Newton's method. A dimensionless time step of $\Delta t = 0.01$ was shown to provide satisfactory numerical convergence as well as sufficient resolution of the time-varying phenomena within the system. A single factorization of the problem with a discretization of 25592 degrees of freedom required approximately 4.8 seconds on a mid-priced PC with a processor speed of 2.0 GHz. For the interested reader, additional details of the model and numerical scheme can be found in [2], [10].

III. Controller Design

The controlled output is chosen to be the spatial average of the meridional kinetic energy, $\mathcal{E}$, a scalar quantity which captures the essential dynamics of the flow within the process,

$$\mathcal{E} = \frac{1}{V}\int_V (v_r^2 + v_z^2)\, dV. \tag{11}$$

The manipulated input is the crucible rotation rate, Ω. To control flows within the vertical Bridgman system, we will derive and implement an input-output linearizing feedback controller. In addition, a conventional proportional and proportional-integral controller will be implemented. All states are assumed to be available from the vertical Bridgman process model.

A. Nonlinear Controller Design

In this work, we design and implement an input-output linearizing feedforward/state feedback controller [11]. A rigorous development of the controller would involve the derivation of an ODE representation of the differential-algebraic equation system resulting from the spatial discretization [12]. Formally, the derivative of the kinetic energy, $\mathcal{E}$, has the form,

$$\frac{2}{V}\int_V \left(v_r \frac{\partial v_r}{dt} + v_z \frac{\partial v_z}{dt} \right) dV, \tag{12}$$

The derivative of the radial component of the velocity vector,

$$\frac{\partial v_r}{\partial t} = -\frac{1}{\mathbf{Pr}_m}[v_r \frac{\partial v_r}{\partial r} - \frac{v_\theta^2}{r} + v_z \frac{\partial v_r}{\partial z}] - (\nabla \cdot \mathsf{T})_r + \mathit{Ra}(T-1)e_z, \tag{13}$$

is dependent upon the crucible rotation rate, through the centrifugal force term, v_θ^2/r. This means that this choice of input-output pair produces a system with a relative order of one. Similarly, the derivative of the kinetic energy is dependent on the furnace temperature profile, through the Boussinesq term, $\mathit{Ra}(T-1)e_z$. Assuming that the controller can measure the disturbance in the temperature field, this results in a system where the relative order of the disturbance is also one. The equal relative orders of the input and disturbance require the use of a static feedforward/state feedback controller to enforce a desired response in the output,

$$\mathcal{E} + \tau \frac{d\mathcal{E}}{dt} = \mathcal{E}_{sp} \tag{14}$$

where τ is the response time constant and $\mathcal{E}_{sp}$ is the kinetic energy setpoint. The control action was calculated numerically by our crystal growth simulation code [10].

B. Proportional and Proportional-Integral Controllers

We also implement a simple, proportional controller,

$$\Omega(t) = K_c\left(\mathcal{E}_{sp} - \mathcal{E}(t)\right) \tag{15}$$

where K_c is the controller gain.

Due to the inverse relationship between rotation rate and kinetic energy, the controller gain is negative. In addition, we implement a proportional-integral controller,

$$\Omega(t) = K_c\left[(\mathcal{E}_{sp} - \mathcal{E}) + \frac{1}{\tau_I}\int_0^t (\mathcal{E}_{sp} - \mathcal{E})\, dt'\right] \tag{16}$$

where τ_I is the controller integral time constant.

IV. Simulation Results

In this work, the primary objective of control is the suppression of flow oscillations arising from a thermal disturbance in the Bridgman furnace.

A. Effect of Steady Crucible Rotation

To begin our analysis, steady-state calculations were conducted for the Bridgman system with furnace reference position, z_r, set to zero. The spatially averaged flow speed was measured as the steady crucible rotation rate, Ω, was varied from zero to 5 rpm. This is shown in Figure 2. The spatially-averaged flow speed is simply the square root of the kinetic energy, $\mathcal{E}$. As seen in the figure, with all other parameters held constant, there is a one-to-one correspondence between rotation rate and flow speed. An increase in rotation rate suppresses the radial and axial components of the velocity field, and consequently the flow speed, with a limiting behavior of solid-body rotation at very high rotation rate (although this limit cannot be

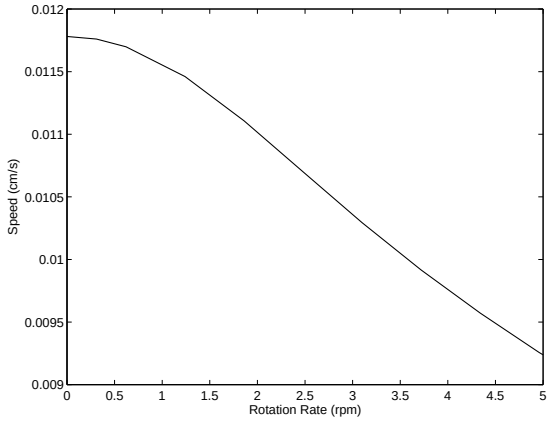

Fig. 2. Steady-state effect of steady rotation on spatially-averaged flow speed.

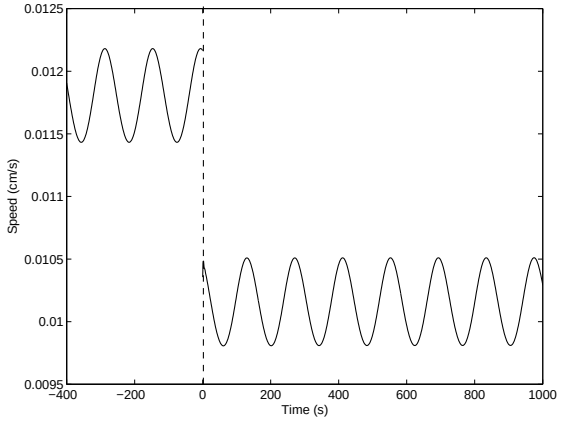

Fig. 3. Effect of steady rotation (Ω = 3.3 rpm) on oscillatory disturbance.

achieved in practice, due to onset of three-dimensional flow instabilities). This behavior, consistent with the results of Yeckel [9], is due to the inhibiting nature of the Coriolis force.

We studied the effect of crucible rotation on the disturbed Bridgman system through transient simulations. Due to buoyancy effects, the sinusoidal variation in the temperature produces a time-varying flow field. Figure 3 shows simulation results when a steady rotation rate of 3.3 rpm is applied to the disturbed system at $t = 0$. It is clear that while steady rotation suppresses the meridional flow, it does not significantly attenuate the disturbance.

B. Closed-loop Results

We now investigate the effect of feedback control on the flows in this system. For all simulations of the disturbed system, the controller setpoint is 1.02×10^{-4} cm^2/s^2, which is equivalent to a spatially-averaged flow speed of 0.0101 cm/s. This setpoint corresponds to a 15% reduction in the speed. Since the application of crucible rotation reduces the kinetic energy of the flow, the setpoint must be chosen at a kinetic energy value less than the steady state kinetic energy corresponding to no rotation ($\Omega = 0$). The data in Figure 2

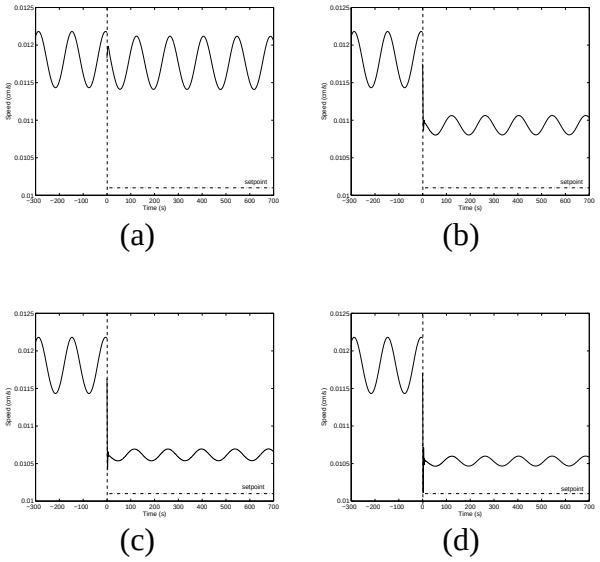

Fig. 4. Proportional Control Simulation Results for K_c = (a) 100; (b) 1000; (c) 2000; (d) 2500: Speed versus Time.

indicate that this setpoint value is physically reasonable. In all simulations, the controller is activated at $t = 0$.

Figures 4 and 5 shows results from P control simulations with controller gains of K_c = 100, 1000, 2000, and 2500. For a small controller gain, proportional control is ineffective: oscillations are hardly suppressed and offset is apparent. As the controller gain is increased, the offset decreases and the oscillations are suppressed with increasing effectiveness. For proportional gains greater than 2500, the closed-loop system becomes unstable.

Figure 5 presents the crucible rotation rates under proportional control using the same four controller gains. At $t = 0^+$, the crucible rotation rate increases sharply from $\Omega = 0$ to the value calculated by the controller algorithm. With increasing controller gain, the initial rotation rate becomes larger to the point of physical infeasibility. This represents an actuator limit which will hinder the practical effectiveness of the P controller. Once the initial transient has passed, thereby establishing the average rotation rate corresponding to the controller gain, the closed-loop system starts to rotate in lock-step with the oscillatory disturbance. Note that the system does not change the direction of rotation; instead it accelerates and decelerates while maintaining the same direction. When the flow speed is relatively large on its oscillation cycle, the rotation rate increases to suppress it. Similarly, when the flow speed is relatively small, the rotation rate decreases.

To eliminate offset, a proportional-integral controller is applied to this system. Simulation results for $K_c = 2000$ and $\tau_I = 1$ are shown in Figure 6. As seen in Fig. 6(a), the PI controller produces melt speeds which oscillate with smaller amplitude and have zero offset. Variation of the integral time constant τ_I has little effect on the long time performance of the controller. The rotation schedule for this

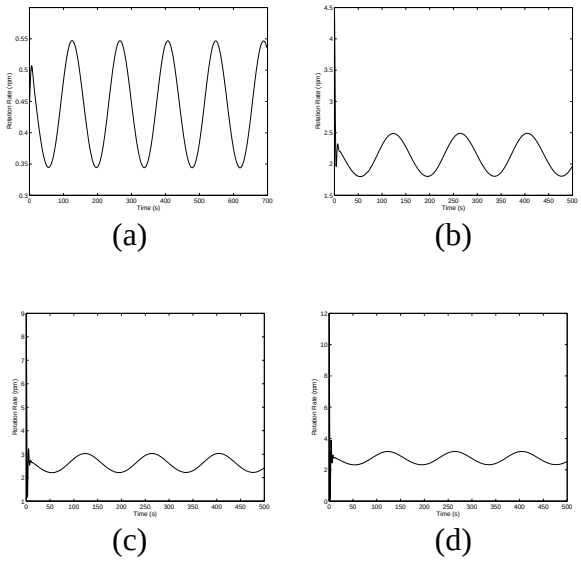

Fig. 5. Proportional Control Simulation Results for K_c = (a) 100; (b) 1000; (c) 2000; (d) 2500: Ω versus Time.

simulation is shown in Fig. 6(b). In a similar manner to P control, the PI algorithm requires that the crucible rotate suddenly and significantly at $t = 0^+$ (see inset).

We now consider the case when nonlinear control is applied to the system. Figure 7 presents closed loop simulation results for time constant $\tau = 1$. As seen in Figure 7, the controller forces a smooth, first-order response to the setpoint, where the oscillations are essentially suppressed. In addition, the nonlinear controller avoids the physically unrealistic actuation spike occurring at $t = 0^+$ in the P and PI control cases. The system accelerates and decelerates in rotation rate to maintain its setpoint.

V. CONCLUDING REMARKS

A prototypical vertical Bridgman system, based on the experimental design of Kim, Witt, and Gatos, was used as the model for feedback controller design and simulation. Proportional control has an inhibiting effect on the sinusoidal disturbance, yet is unable to fully suppress oscillations or obtain zero offset in the output. As expected, proportional-integral control improved the closed-loop performance, suppressing oscillations considerably and providing zero offset. To obtain adequate oscillation suppression, both the P and PI controllers required extremely aggressive controller action at the onset of control. This actuation spike would likely cause practical problems. In contrast to these simple controllers, the nonlinear model-based controller provided a smooth transition from the initial state (zero rotation rate) to the final state (non-zero, time-varying rotation rate). Also, the nonlinear controller provided improved oscillation suppression as compared with the linear controllers. These simulations demonstrate that feedback control can be used in conjunction with crucible rotation to effectively modify the flows in a vertical Bridgman crystal growth system.

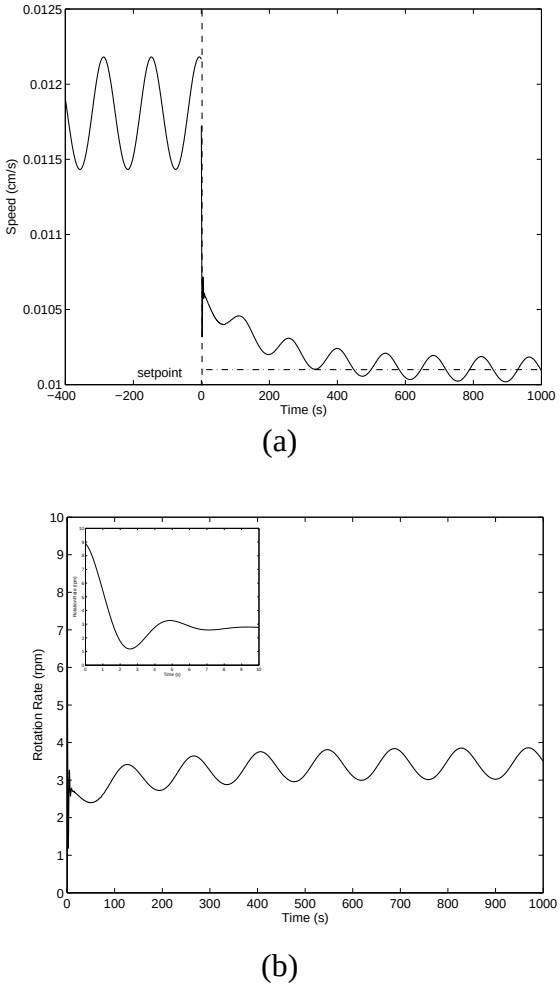

Fig. 6. PI Control Simulation Results for $K_c = 2000$ and $\tau_I = 1$: (a) Speed versus Time; (b) Ω versus Time.

Issues remain with the practical application of control to the vertical Bridgman system. Due to the use of an enclosed crucible, and the need to conduct growth inside a high temperature furnace, it is extremely difficult to measure the states during growth. In practice, flow states could be related to thermocouple measurements, as done by Kim, Witt, and Gatos [1]. Other feasible techniques include estimation by eddy sensors, or by detailed crystal growth models. This will be the subject of future research. We are also currently investigating other actuation methods for flow control. These methods include thermal profile adjustment, either globally via the furnace or pointwise using lasers, application of magnetic fields, or crucible vibration.

VI. ACKNOWLEDGMENTS

Partial support of this work from grant NSF/CTS-0201486 is also gratefully acknowledged. Computing resources were provided by the University of Minnesota Supercomputing Institute. PS would also like to acknowledge support from a Doctoral Disseration Fellowship awarded by the University of Minnesota.

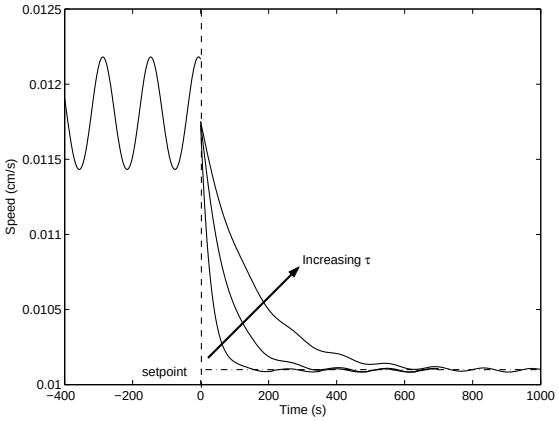

(a)

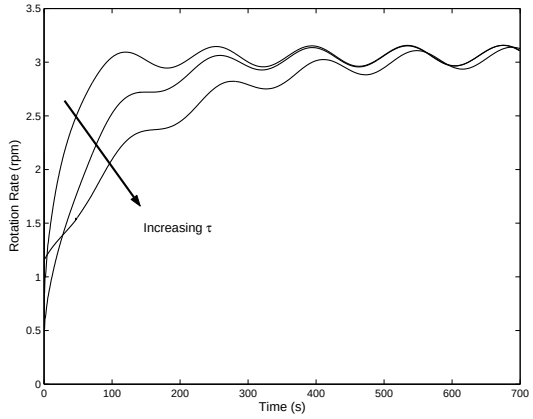

(b)

Fig. 7. Nonlinear Control Simulation Results for $\tau = 1$: (a) Speed versus Time; (b) Ω versus Time.

REFERENCES

[1] K.M. Kim, A.F. Witt and H.C. Gatos, Crystal Growth from the Melt under Destabilizing Thermal Gradients, *J. Electrochem Soc.*, vol. 119, 1972, pp 1218-26.

[2] P. Sonda, PhD Thesis, The Modeling, Simulation, and Control of Transport Phenomena in a Thermally Destabilizing Bridgman Crystal Growth System, 2003.

[3] P. Sonda, A. Yeckel, P. Daoutidis and J.J. Derby, Improved radial segregation via the destabilizing vertical Bridgman configuration, *J. Crys. Growth*, vol. 260, 2004, pp 263-276.

[4] C. Batur et al., On-line control of solid-liquid interface by state feedback, *J. Crys. Growth*, vol. 205, 1999, pp 395-409.

[5] A. Srinivasan et al., Solid-liquid interface shape control during crystal growth, *Proceedings of the 1995 American Control Conference*, vol. 2, 1995, pp 1270-4.

[6] Y. Azuma et al., Growth of SiGe bulk crystals with uniform composition by utilizing feedback control system of the crystal-melt interface position for precise control of the growth temperature, *J. Crys. Growth*, vol. 250, 2003, pp 298-304.

[7] M. Schmachtl, A. Schievenbusch, C. Zimmerman and W. Grill, Crystallization process control during directional solidification in a high-temperature-gradient furnace by guided ultrasonic waves and real-time signal evaluation , *Ultrasonics*, vol. 36, 1998, pp 291-5.

[8] P. Capper and J.J.G Gosney, Application of the accelerated crucible rotation technique to the Bridgman growth of CdHgTe: simulations and crystal growth, *J. Crys. Growth*, vol. 70, 1984, pp 356-64.

[9] A. Yeckel and J.J. Derby, Effect of Accelerated crucible rotation on melt composition in high-pressure vertical Bridgman growth of cadmium zinc telluride, *J. Crys. Growth*, vol. 209, 2000, pp 734-50.

[10] A. Yeckel and R. Goodwin, *Cats2D (Crystallization and Transport Simulator), User Manual*, Unpublished (available at http://www.msi.umn.edu/∼yeckel/cats2d.html); 2003.

[11] P. Daoutidis and C. Kravaris, Synthesis of feedforward/state feedback controllers for nonlinear processes, *AIChE J.*, vol. 35, 1989, pp 1602-15.

[12] A. Kumar and P. Daoutidis, *Control of nonlinear differential algebraic equation systems*, Chapman and Hall, London; 1999.